

ENABLING TECHNOLOGIES

Synchrotron phase-contrast X-ray imaging reveals fluid dosing dynamics for gene transfer into mouse airways

M Donnelley^{1,2,3}, KKW Siu^{4,5,6}, RA Jamison⁷ and DW Parsons^{1,2,3,8}

Although airway gene transfer research in mouse models relies on bolus fluid dosing into the nose or trachea, the dynamics and immediate fate of delivered gene transfer agents are poorly understood. In particular, this is because there are no *in vivo* methods able to accurately visualize the movement of fluid in small airways of intact animals. Using synchrotron phase-contrast X-ray imaging, we show that the fate of surrogate fluid doses delivered into live mouse airways can now be accurately and non-invasively monitored with high spatial and temporal resolution. This new imaging approach can help explain the non-homogenous distributions of gene expression observed in nasal airway gene transfer studies, suggests that substantial dose losses may occur at delivery into mouse trachea via immediate retrograde fluid motion and shows the influence of the speed of bolus delivery on the relative targeting of conducting and deeper lung airways. These findings provide insight into some of the factors that can influence gene expression *in vivo*, and this method provides a new approach to documenting and analyzing dose delivery in small-animal models.

Gene Therapy (2012) 19, 8–14; doi:10.1038/gt.2011.80; published online 9 June 2011

Keywords: X-ray imaging; high resolution; mouse; airways; instillation; gene transfer

INTRODUCTION

The mouse respiratory system is widely used for the modeling of disease and treatment using live pathogens (bacterial, viral and fungal), pollutant particles, pharmaceuticals, allergens and gene therapies. Our group uses the mouse nose and lung as *in vivo* model sites for developing a gene therapy treatment for cystic fibrosis (CF) airway disease.^{1,2} Reporter genes and/or the therapeutic (CFTR) gene contained in a lentiviral gene vector are delivered by *in vivo* bolus instillation into the nose and trachea. To produce lasting gene expression after a single dose event we utilize a 4 μ l 0.1–1% (typically 0.3%) lysophosphatidylcholine (LPC) airway pre-treatment before delivering a 20 μ l lentiviral gene vector dose (typically 10^7 – 10^9 tu ml⁻¹) to the mouse nose.^{1–4} Reliable dosing is essential for the success of these airway gene transfer protocols, but despite the use of standardized delivery techniques our group and others report large variability in reporter gene histological assessments and in electrophysiological gene transfer measurements.^{2,5,6} One cause of this variability may be the heterogeneous dose distribution that may occur in the physically complex nose and trachea.

The ability of standard imaging modalities to visualize the fluid dynamics in the mouse nose and lung is limited by their spatial and temporal resolution and their poor ability to discriminate soft tissues from air-containing structures in two-dimensional imaging modes. Small-animal computed tomography, and to a lesser extent magnetic resonance imaging, which provide three-dimensional information via tomographic approaches, could be used to examine murine airways but the time to acquire three-dimensional data sets prohibits tracking

of high-speed dynamic events such as fluid dosing at high spatial resolutions. Although positron emission tomography has been used to show the final location of transnasally delivered solutions,⁷ the acquisition speed and spatial resolution of positron emission tomography is very low, the dynamics of the fluid delivery cannot be imaged, the air-containing spaces are poorly defined and the spatial resolution is insufficient. None of these methods can visualize fluid movement in mouse airways at high resolution.

Synchrotron phase-contrast X-ray imaging (PCXI)^{8,9} is able to monitor the fate of a fluid dose bolus—similar to those used in our gene transfer studies—in the time immediately after delivery with high temporal and spatial resolution. Synchrotron X-rays are electromagnetic radiation generated by the acceleration of ultra-relativistic (that is, close to the speed of light) electrons through magnetic fields. PCXI provides enhanced image contrast by utilizing X-ray refraction in addition to conventional X-ray absorption and is particularly useful for achieving soft tissue contrast even where the absorption differences are small. The technique requires a spatially coherent source of X-rays, which is readily achievable using a synchrotron due to its intrinsically small source size. Tissue/air boundaries in particular are enhanced by the phase changes induced by their differences in X-ray refractive indices.^{8,9} We have previously demonstrated the advantages of PCXI for small-animal airway-surface imaging^{10,11} and for monitoring the post-deposition behavior of particulates on live mouse nasal and tracheal airways.^{12,13} In this study, we used PCXI to precisely and non-invasively track how

¹Department of Respiratory and Sleep Medicine, Women's and Children's Hospital, Adelaide, Australia; ²Centre for Stem Cell Research, University of Adelaide, Adelaide, Australia;

³Department of Paediatrics and Reproductive Health, University of Adelaide, Adelaide, Australia; ⁴Monash Biomedical Imaging, Monash University, Clayton, Victoria, Australia;

⁵School of Physics, Monash University, Clayton, Victoria, Australia; ⁶Australian Synchrotron, Clayton, Victoria, Australia; ⁷Division of Biological Engineering, Monash University,

Monash, Victoria, Australia and ⁸Women's and Children's Health Research Institute, Adelaide, Australia

Correspondence: Dr M Donnelley, Department of Respiratory and Sleep Medicine, Women's and Children's Hospital, 72 King William Road, North Adelaide, SA 5006, Australia.

E-mail: martin.donnelley@adelaide.edu.au

Received 19 December 2010; revised 29 April 2011; accepted 3 May 2011; published online 9 June 2011

introduced fluids, typical of those used in airway dosing, move through the airways of live and intact small animals.

We hypothesized that the effectiveness of the initial targeting and the distribution of a dose in live mouse airways could be determined for the first time by recording the immediate fate of instilled fluids in the nose and trachea. This study showed that the spread of the dose, the effectiveness of the delivery method and the persistence of the delivered dose could be visualized. Furthermore, the effects of altered dose volume and speed of delivery were also visible. This method now enables the rational design of more effective delivery procedures in the airway gene transfer protocols used in normal and CF mouse models.^{1,2,14,15} It should also permit improvements in reliability and repeatability to boost outcome effectiveness, reduce outcome variability and decrease the volumes of costly gene vectors needed in mouse model studies.

RESULTS

No methods have been available to show the detailed fate of gene therapy fluid doses in the period immediately after delivery into mouse nose or trachea. The primary advance here was the coupling of an iso-osmotic iodine-based contrast fluid, mimicking our gene transfer dosing protocol, with synchrotron PCXI. Together they enabled direct and non-invasive visualization of the dynamics of the fluid delivery at a resolution that permitted reliable identification of the specific airway anatomy and regions affected. PCXI also provided unambiguous visualization of the complexity of the targeted nasal airways and trachea,¹⁰ while also enhancing the boundary between the air and instilled contrast medium. We utilized a remote delivery apparatus to provide reliable initiation and duration of dosing and found that the 1:1 mixture of water and contrast fluid was well tolerated by the anesthetized mice. Only occasional respiratory perturbations occurred with the large volume deliveries, at a similar incidence to that experienced during our gene transfer studies.

During the experiments, the incident photon flux was $\sim 1.5 \times 10^8$ photons per sec per mm^2 , producing a radiation dose of ~ 2 mGy for each 100 ms exposure. To the mouse this dose is comparable to a single human skull X-ray.¹⁶

Nasal dose delivery

Figure 1 shows the position of the instilled $4 \mu\text{l}$ dose (a surrogate for our LPC pre-treatment) in six different mice 10 s after the completion of the standard 10 s fluid delivery. The pseudo-coloring shows where contrast fluid is present in the nasal airway and is created from the difference in contrast between the current and pre-delivery image frames. Fluid was taken up into the airway via normal tidal breathing, as occurs in our gene transfer dosing protocols. It is apparent that mice N1–N4 show a very similar fluid distribution pattern in the lateral and posterior regions of the right nasal cavity. Compared with the anterior nostril region, far less fluid reaches the edge of the centrally placed septum than moves laterally. Note that in mouse N3, fluid is also present along the lateral edge of the right airway and the amount of lateral right-nostril fluid is reduced. Supplementary Video 1 shows the spread of fluid within the nasal airways of all six mice as the dose is progressively expelled from the nearby cannula. Two mice (N5 and N6 in Figure 1) show the effect of incomplete nasal dose deliveries, caused by an adherent fluid droplet forming at the cannula tip. In mouse N6, the droplet bridges across to the nostril and is suddenly inhaled, immediately extending the distribution of fluid into the right nasal cavity. In mouse N5, the droplet remains at the tip throughout (see also Figure 2 below, where the fluid droplet is still present 10 min later); this lower delivered volume prevented fluid reaching the more posterior regions of the right nasal airway when compared with mice N1, N2 and N4. In mouse N3, some fluid traveled along the right side of the nasopharyngeal meatus, causing a reduction in the dose retained within the right nasal anterior airway. Despite the variability, fluid was still present in the nasal cavities of all mice 10 min after the initial $4 \mu\text{l}$ delivery.

Figure 2 shows the effects of a subsequent $20 \mu\text{l}$ dose (a surrogate for our lentiviral vector) delivered into the same mice (N1–N5). Images were processed such that the contrast fluid remaining 10 min after the $4 \mu\text{l}$ delivery was considered to be background, enabling the dynamics of this second dose bolus to be easily seen. These images show a wider dose distribution extending into the nasopharynx and past the epiglottis, as might be expected from addition of a larger dose. The dynamics of this second dose delivery are shown in Supplementary

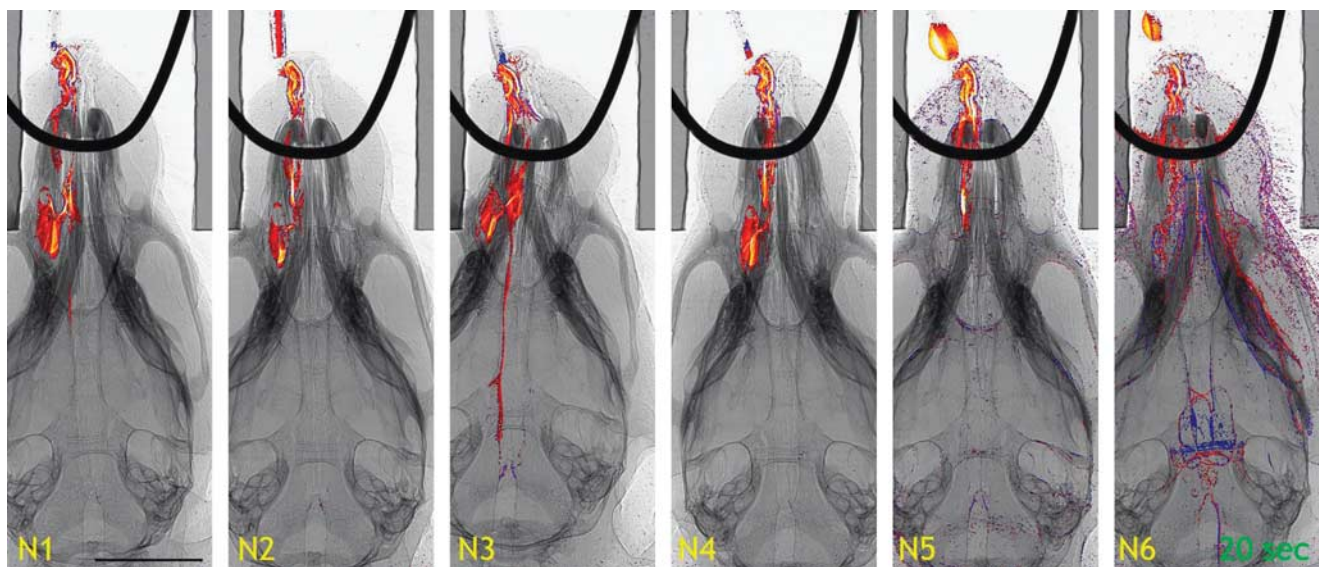


Figure 1 Four microliter fluid dose in mouse nasal airways. Pseudo-colored images from the background subtraction algorithm showing the location of a $4 \mu\text{l}$ delivered dose of 1:1 iomeprol and water mix delivered over 10 s in six mice. Each image shows the fluid distribution 20 s after delivery initiation. Scale bar is 5 mm in all figures.

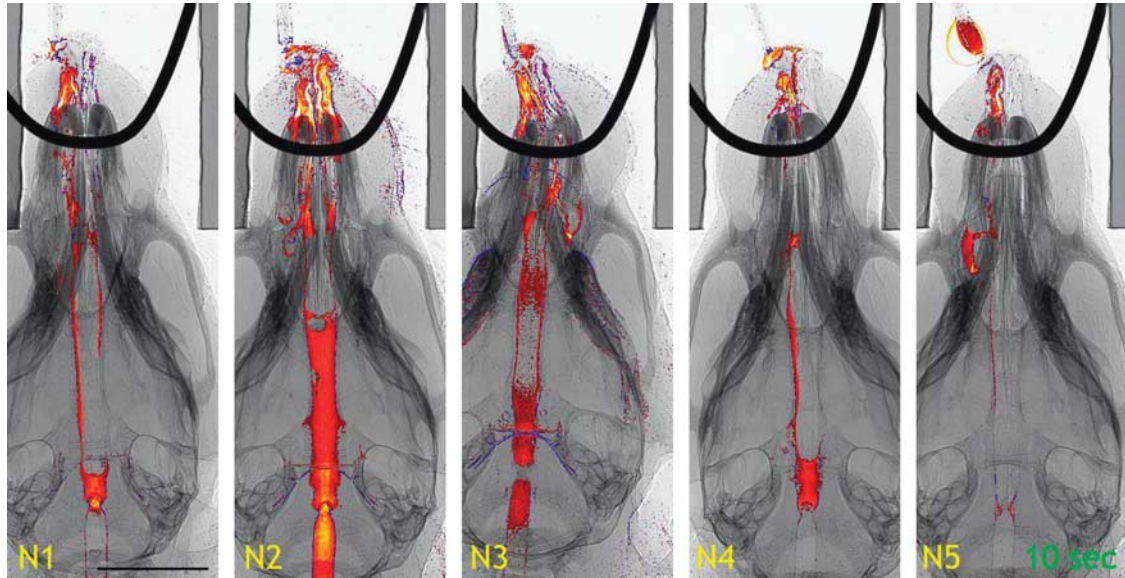


Figure 2 Twenty microliter fluid dose in mouse nasal airways. Images from five mice (mouse N6 in Figure 1 died of unknown causes while under anesthesia just before this dose delivery), showing the location of a 20 μ l dose that was delivered over 30 s. The images are taken at 10 s after delivery began.

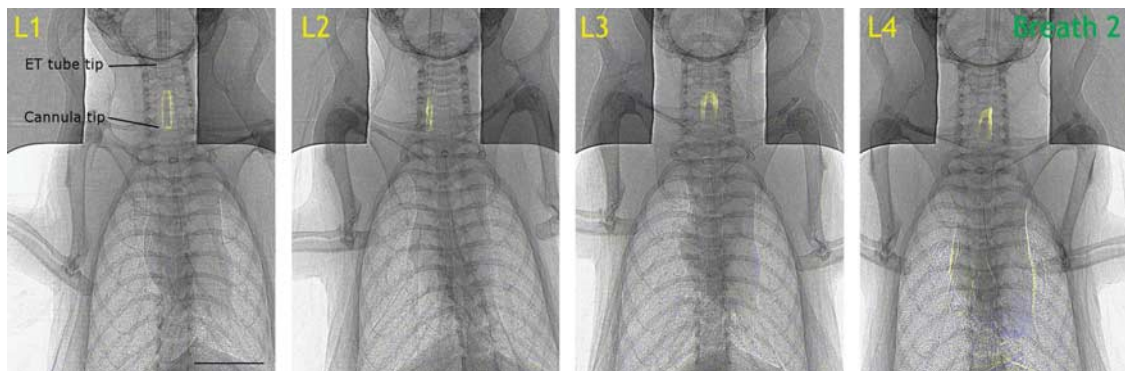


Figure 3 Fifteen microliter fluid dose in mouse trachea. Images from the frame difference algorithm showing the location of the initiation of a 15 μ l dose delivered slowly over 30 s (shown at two breaths after delivery initiation in four mice). The location of the cannula tip and ET tube tip are marked for mouse L1. Images are taken from Supplementary Video 3.

Video 2. We were surprised to observe the extensive and rapid filling of the nasopharyngeal meatus, the cyclical nature of bulk fluid movement up and down the nasal airway, the creation of both small and full-width gas bubbles and the ability of this 20 μ l dose to pass the epiglottis and enter the trachea. In addition, some fluid also reaches into the pharynx and the oral cavity where it is evident as large bubble edges that are wider than the boundaries of the posterior nasopharyngeal airway. This is best observed in some of the later image frames for mouse N2. Cessations of nasal airway fluid movement in these spontaneously respiring mice were also noted after the 20 μ l dose, visible as almost stationary airway bubbles, air gaps or fluid within the nasopharynx across a number of frames in mice N1 (25–53 s), N2 (14–32 s) and N3 (16–57 s) in Supplementary Video 2.

Lung dose delivery

The captured image frames required different processing to the nasal airway images. We displayed the fluid position (in yellow–blue pseudo-color) by calculating the intensity change *between* frames, thereby minimizing the effects of any general body and lung

movement throughout the experiment (see Supplementary Video 3). Figure 3 shows where instilled fluid was present two breaths (2.25 s) after the initiation of a 30 s delivery of 15 μ l of fluid via the dosing cannula. For clarity, the tips of the endotracheal (ET) tube and the smaller diameter dosing cannula are both marked in one mouse (L1). Of particular note is the immediate retrograde movement of the fluid from the cannula tip in each animal (see breaths zero to eight in Supplementary Video 3), although the manner of movement was different. For example, in mouse L1, the dose tracked back along the cannula outer wall; in mice L2 and L4, fluid also spread onto one side the tracheal wall; and in mouse L3, fluid spread to both tracheal walls. Figure 4 shows an example of the dynamics of lung fluid delivery (images were captured at 1.33 Hz from mouse L1 in Figure 3, and were extracted from Supplementary Video 3), as a portion of the fluid dose moves down the left main bronchus.

To determine how a faster delivery rate affected the distribution dynamics, we delivered the same 15 μ l volume over a 3.6 s period, the maximum flow rate of the infusion pump (Figure 5). This fast fluid bolus delivery (images in Figure 5 extracted from Supplementary

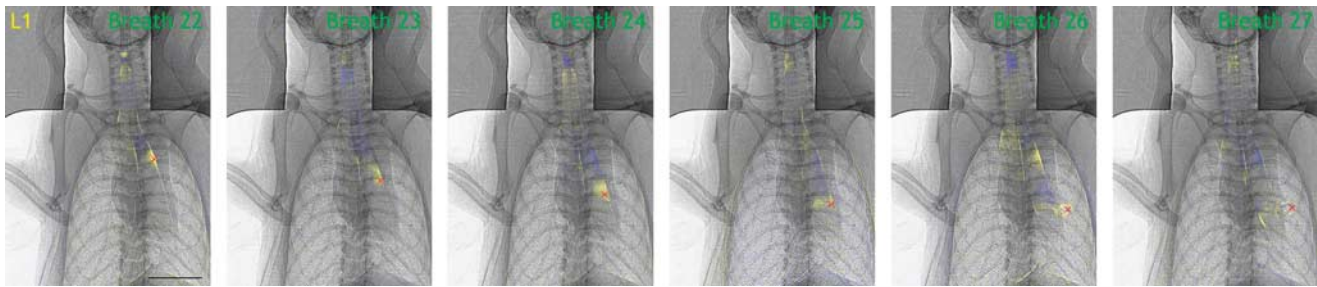


Figure 4 Fluid movement in lung conducting airways. Six breaths from one mouse (L1 in Figure 5, which received 15 μ l of fluid over 30 s) starting 22 breaths after dose initiation, showing a bolus of fluid, marked with a red X, moving down the left main bronchus.

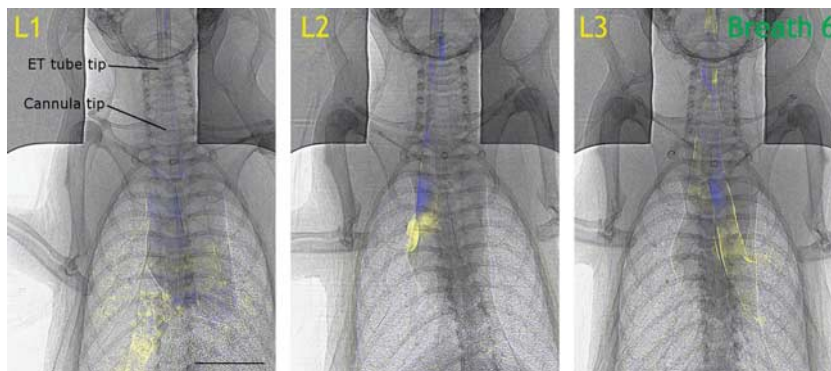


Figure 5 Fifteen microliter fluid dose rapidly delivered into mouse trachea. The location of the initiation of a 15 μ l dose delivered quickly over 3.6 s (shown at six breaths after delivery initiation, that is, \sim 1 s after delivery ceased). The location of the cannula tip and ET tube tip are marked for mouse L1. Only three mice are shown for the fast delivery, mouse L4 in was not imaged due to technical issues. Images are taken from Supplementary Video 4.

Video 4) created larger localized increases in the contrast fluid volume that were more easily visualized. The video sequences show localized boluses progressing along both the left and right main bronchi. The ensuing spread of the contrast bolus into bases of the respective lung lobes is shown by the rapid loss of contrast, probably due to splitting of the bolus into smaller airways in the base of this lobe. This faster dosing method clearly delivered more fluid more rapidly into the small airways of the lung lobes than the slower delivery.

Although the entire lung perturbations or small body movements could interfere with image analysis of dose delivery, they also show a direct effect of instilling fluid into a mouse airway. The small movements in the alveolar speckle pattern (which is greatly enhanced by PCXI)¹⁷ during normal respiration, as well as movement of the heart muscle, are sufficient to often partially obscure the movement of the contrast agent in airways. In some animals, such as mouse L3, the body movements were large enough to create ‘ghost’ outlines of bones and organs, since the pseudo-color processing highlights all differences between frames (for example mouse L3, breaths 18, 41 and 58 in Supplementary Video 3).

DISCUSSION

The primary goal of this study was to document and understand the dynamics of fluid bolus dose delivery into the nose and trachea of live mice using synchrotron PCXI. This is the first method we are aware of able to provide high-resolution non-invasive imaging of dosing dynamics in live intact mice. It has the potential to improve the effectiveness and reduce the variability of gene therapy protocols where despite standardized procedures inconsistent levels and

distributions of cell transduction are experienced in mouse nose and lung.^{1,2,4} This new ability to directly visualize the delivery of a fluid in the airway at high temporal and spatial detail also suggests an immediate relevance and utility to other respiratory health and disease research modeling applications in small animals when pharmaceutical, infectious, allergenic and particulate fluid installations are utilized.

This PCXI data can now help explain some of the patterns of gene expression produced by our gene transduction protocols in living mouse airways. Only the nasal epithelium in transgenic CF mice is suited to CF airway gene transfer modeling¹⁸; in our studies we utilize a 4 μ l LPC pre-treatment followed by a 20 μ l lentiviral vector dose.¹⁻⁴ When correctly delivered (Figure 1, mice N1 and N2), the 4 μ l volume remained on the treated side of the nasal cavity. In mouse N3, fluid can also be seen in the nasopharynx, but only along the treated side of the nasal airway. These results validate the use of a 4 μ l dose (originally estimated by scaling down dose volumes established in rats¹⁹ based on typical mouse body weights) to dose one anterior nasal airway while simultaneously retaining an untreated (left) nasal airway to act as an unexposed, within-animal control airway for nasal airway studies. Furthermore, the results suggest that in those rare cases where gene expression extended into the nasopharynx (see Limberis *et al.*⁴ and the cover photo of that issue), the expression was limited to the treated side, that is only to those areas where the 4 μ l LPC pre-treatment had reached. The retention (rather than rapid loss) of a 4 μ l dose within both the respiratory and olfactory epithelial regions of the treated nostril supports, first, the strength and reliability of gene expression we have observed in nasal ciliated epithelium. Second, it suggests that the absence of transduced (non-target) olfactory

epithelium from our vesicular stomatitis virus G pseudo-typed lentiviral gene vector^{2,4} occurs despite the vector dose distributing into and being retained in this mixed transitional/olfactory region. This distribution is also consistent with the off-target transduction of olfactory tissue produced by other vectors (for example AdV, FIV, etc).^{14,20} Finally, the lower levels of gene expression we observe on the nasal septum compared with the lateral ciliated regions are consistent with the differences in fluid retention in these two regions. The ability to observe where the dose is retained, or the tissue-type targeted,²¹ should be useful in the testing of pharmaceuticals, infectious agents, allergens and other gene vectors in these different epithelial tissues. The visualization of partial dose delivery distributions also suggests that whenever incomplete or inconsistent dosing (for example nostril bridging or sneezing) is noted, gene transduction is likely to be affected. One recommendation from these findings is that to reduce outcome variability of those animals that show partial dosing and/or sneezing or snorting of the dose should not be included in normal assessments.

The 20 μ l nasal dose (equal to our lentiviral gene vector delivery volume) appears to overwhelm the 'holding capacity' of the pre-treated anterior right-nostril region; this second nasal airway fluid delivery moved immediately into the nasopharynx. Supplementary Video 2 reveals a reciprocating fluid motion in some mice, with some fluid continuing past the epiglottis into the trachea. Although the anatomy below the upper trachea could not be imaged in this nasal airway study, it is likely that fluid reached further into the lung airways, a finding consistent with a recent low-resolution radiotracer study.⁷ The results also support our finding that long-term gene expression was produced in the lung by a lentiviral vector containing the luciferase transgene that was delivered to the nose and was designed specifically to produce *nasal* airway gene transfer.²² It follows that smaller gene vector doses might be able to produce the same levels of gene expression in the anterior nasal airways.

Comparison of the distributions of the 4 and 20 μ l volumes also supports the proposed mechanism of action of LPC pre-treatments. If LPC makes the airway-surface receptive to gene vector uptake,³ we expect that vector transduction will only occur where LPC has previously reached and affected an airway-surface region. The unilateral nasal airway gene expression produced when using these protocols^{2,4} is consistent with this notion since we only observe patterns of gene expression in areas reached by the 4 μ l dose, despite demonstrating the wide reach of the 20 μ l (surrogate vector) dose throughout the entire nasopharynx. The nasopharynx epithelium is entirely ciliated respiratory epithelium²¹ and it follows that if the nasopharynx could be effectively pre-treated around its full circumference with LPC, then homogeneous gene transduction might be achieved there. This novel lung airway-like site could potentially be used for modeling the effects of gene vectors or drugs on ciliated airway function within a tubular lung-like conducting airway, an option identified by others in related studies of mouse nasal electrophysiological function.²³ It should be noted that once fluid reaches the nasopharynx in sufficient volume to fill the airway diameter, it is possible for retrograde fluid movement into the contralateral anterior nasal airway due to normal breathing or 'sneezing' reactions that produce fluid movement into otherwise un-dosed airway regions.

Although most CF airway gene therapy research in mice is based on effects in ciliated nasal airway tissue,¹⁸ most murine respiratory research is naturally focused on the trachea, conducting airways and parenchyma. The current study showed how the speed of delivery can alter the way a fluid dose spreads into the lung tree. Although mice were oriented vertically, the fluid was observed moving into the left,

the right or into both mainstem bronchi despite a standard dose-delivery protocol via an accurately placed tracheal dosing cannula. Of some note is that the first movement of fluid after it was slowly expelled from the cannula was retrograde, away from rather than down into the lung. The instilled fluid moved out of the airway against gravity, along or around the cannula body and/or on the adjacent tracheal wall, therefore reducing the intended volume delivered to the targeted distal conducting airways and parenchyma. The studies here were not designed to quantify these losses, but it is clear that it is important to monitor and document dose losses during lung instillations, since such losses may help explain the patchy gene expression distribution and the high variability we and others observe in lung dosing studies.

This new imaging method is broadly applicable. It now permits evidence-based attention to the design of mouse lung dosing protocols to improve the delivery to specific regions of the lung, for example, by linking the effect of incomplete dosing to its reach into regional airways. It could also reveal how a defined smaller dose might be effectively targeted to more restricted regions of anterior nasal airway. More generally, it has the ability to provide an accurate and direct correlation between the effect of the delivery of a treatment dose and its outcome. The variations in outcome that result from changes in cannula placement, dose volume, timing of delivery (initiation of, and during the respiratory cycle), orientation of the mouse and the speed of delivery could also be assessed using this technique.

The lung is a challenging organ to image accurately and precisely. Accurate detection of fluid motion in airways requires the regions of interest to be motionless, but for lung imaging this must be traded against the need to leave the lung structural elements free to move with respiration. Muscle paralysis agents were not employed here, and although gating image acquisition to the respiratory cycle was usually effective, this alone did not accommodate the small variations imposed on the rates of expansion or contraction of the lung, especially when these were perturbed by the fluid dosing itself. A 20 μ l fluid dose introduced into a lung of ~ 300 μ l tidal volume (an $\sim 6.7\%$ volume change) sufficiently perturbed the regularity of the ventilator-driven lung movement such that all the lung lobes (for example, mouse L1 in Supplementary Video 4) were strongly pseudo-colored, complicating data analysis and interpretation.

The large field of view and high resolution of the SPring-8 BL20B2 beamline affords a unique view of how a dosing fluid moves in a live intact respiratory system. In these experiments, we chose to image at a low frame rate (1 Hz for the free breathing nasal studies, and at 1.33 Hz for lung as triggered by the ventilator) but in a separate study (data not shown) we have already imaged mouse lungs at nearly 30 Hz, sufficient to capture all stages of the respiratory cycle. Clearly, this new approach greatly improves on the capabilities of currently available imaging modalities in live animals both in terms of its spatial and temporal resolution, and in the ability to better visualize the air-containing anatomical structures. These capabilities provide considerably more imaging possibilities than systems utilizing a radio-tracer,⁷ which are substantially limited by the capture period (that is, 40 s per frame) and spatial resolution (that is, 0.81 mm isotropic voxels, 50 times larger than the pixel size used here). Since the radiation dose for a single image acquired during this experiment was $<2\%$ of the total dose delivered in a single small-animal micro-computed tomography scan,^{24,25} this technique has the potential to be applied to studies designed to correlate how alterations in fluid dose delivery parameters can affect subsequent gene expression.

There are limitations that, when addressed in future studies, should further expand the potential of this technique. Mice were only

oriented vertically (that is, head high) here to match our current mouse airway gene transfer protocols,^{2,4} providing a standard orientation and direct (or stereomicroscope) vision of cannula-based delivery to the nostril. However, there are a range of animal orientations used by other research groups,²⁶ and since orientation is a likely contributor to the diversity of outcomes of nasal airway gene transfer, this technique can now provide precise comparisons of the effect of body orientation on dose-fluid distributions. The use of paralytic agents should also be considered to better limit confounding lung and body movements. Our method can also be used to ask similar questions in pollutant, allergen and infectious-agent studies in mouse lung. It may also assist in defining dose-delivery protocols better able to direct a dose to specific regions or lobes of the lung without introducing the confounding effects that potentially arise from deep cannula placement into airways, such as we have observed in gene transfer studies (see Liu *et al.*,¹ Figures 1e and f).

Although we diluted the contrast fluid to make it iso-osmotic with physiological saline, the delivered fluid had a slightly higher viscosity than isotonic sodium chloride.^{27,28} In addition, the complex non-Newtonian properties and behavior of a two-phase viral gene vector may not be accurately mimicked by a single phase contrast agent. However, since each gene vector can have a different viscosity due to the influence of the diluent, the level of included proteins, and the concentration of vector particles, the viscosity is a characteristic that should be examined when considering the progression and intended destination of a dose moving through small airways where capillary forces issues may be significant. Since the viscosity affects the vector residence time,^{29,30} and therefore the level of gene transduction, the effect of this key characteristic may now be quantified using this technique.

In summary, this non-invasive high-resolution synchrotron PCXI technique for visualizing and analyzing fluid dose movement has for the first time provided gene therapy researchers the ability to ask and answer specific questions about the airway distribution dynamics of fluid doses delivered into live mouse nose and trachea. In a number of small-animal models, it could allow creation of standardized dosing protocols able to maximize and compare outcomes across different research groups while using the most appropriate volume of expensive gene vectors or other pharmaceutical agents.

MATERIALS AND METHODS

Experiments were performed on the BL20B2 bending magnet beamline at the SPring-8 synchrotron radiation facility in Japan, under approvals from the Animal Ethics Committee of SPring-8, and of the Child, Youth and Women's Health Service, Adelaide. Mice were anesthetized with pentobarbital (Somnopentil, Pitman-Moore, Washington Crossing, PA, USA; 100 mg kg⁻¹ i.p.) and then anesthesia was maintained by constant infusion of Nembutal (0.1 mg kg⁻¹ per second, via an indwelling i.p. needle) from a syringe pump (UltraMicroPump III and Micro4 controller, World Precision Instruments, Sarasota, FL, USA). Body temperature was maintained using an infrared heat lamp and monitored with a rectal thermometer. Mice were anesthetized for a total of <1 h. After completion of each experiment, mice were humanely killed via overdose of pentobarbital, without loss of anesthesia. Since mice remained anesthetized before death, no attempt was made to minimize radiation dose, rather we maximized both the number and quality of the images acquired.

Imaging setup

The imaging hutch was located in the Biomedical Imaging Centre, 211 m from the source,³¹ and the imaging layout was as described previously.¹⁰ Monochromatic 25 keV ($\lambda=0.5 \text{ \AA}$) X-rays were selected using a Si(111) double-crystal monochromator to provide maximum flux at this energy.³² A propagation (sample to detector) distance of $\sim 2 \text{ m}$ was chosen to produce optimal phase

contrast for airway imaging. X-rays were converted to visible light using a P43 (Gd₂O₂S:Tb) scintillator and images were captured using a CCD detector (C9300-124F21, Hamamatsu Photonics, Hamamatsu City, Shizuoka Prefecture, Japan) coupled to the scintillator using a fiber optic taper. The CCD detector had an array size of 4000×2672 pixels and a 9×9 μm² native pixel size. This setup resulted in an effective isotropic pixel size of 16.2 μm. A subarray of the CCD (1648×1936 pixels) was matched to the beam size at the sample position to give a field of view of $\sim 27 \times 31 \text{ mm}^2$. An exposure length of 100 ms was chosen to capture sufficient photons to fill the potential dynamic range (2¹² gray levels) of the detector, provide the maximal signal-to-noise ratio without detector saturation and minimize blurring from animal movement.

Nasal studies

Six anesthetized female C57/Bl6 mice ($\sim 20 \text{ g}$) were individually secured head-high to a polyethylene imaging board³³ with the incisors hooked over a wire loop and the limbs, shoulders and lateral torso taped to the board to minimize body movements. The imaging area (head/torso) was brushed with a thin layer of glycerol to eliminate air in the fur layer (which would otherwise create a high signal in the images as PCXI is very sensitive to boundaries). The X-ray beam passed dorso-ventrally through the nose (and the lung, see below). A PE10 polyethylene cannula (SteriHealth, Melbourne, Australia) was positioned using a micromanipulator so its tip was 1–2 mm above the right nostril, to simulate our normal (hand-delivered) nasal gene vector delivery setup.¹ A 1:1 mix of the iodine-based contrast agent iomeprol (Iomeron 350, Bracco-Eisai, Tokyo, Japan²⁸) and water (to produce an osmolarity similar to 0.9% saline) was delivered through the cannula using a second UltraMicroPump III syringe pump, remotely activated from outside the imaging hutch. Priming of the syringe and PE tubing ensured accurate dose initiation and delivery. Fluid was taken into each mouse by its normal tidal volume inhalations and the cannula tip did not make contact with the mouse.

Images were captured at 1 Hz. After 1 min of baseline collection, a 4 μl sample of the contrast mix (as a surrogate for our 4 μl gene transfer airway pretreatment protocol)^{2–4} was delivered in a single bolus over 10 s. Following 10 min of data collection, an additional bolus of 20 μl (a surrogate for gene vector delivery) was delivered over 30 s. Image capture continued for a further 10 min, creating a 21 min data set consisting of a total of 1260 images per mouse covering two acute dose deliveries.

Lung studies

A similar protocol was used for the lung imaging. Four female C57/Bl6 mice ($\sim 20 \text{ g}$) were anesthetized then intubated with a 20 Ga i.v. catheter (Insyte, Becton Dickinson, UT, USA).³³ This ET tube was inserted into the trachea to a nominal depth of 22.5 mm from the nose tip, which placed the ET tube tip below the fifth cartilage ring (approximately half way between the epiglottis and the carina). The Luer hub of the catheter was immediately cut off to enable the ET tube to be directly connected to the ventilator circuit and ensure respiratory dead-space was minimized. A flexiVent small-animal ventilator (Scireq, Montreal, Quebec, Canada) provided ventilation set at 80 breaths per min, with a tidal volume of 30 ml kg⁻¹ (minute ventilation $\sim 48 \text{ ml per minute}$) and $\sim 3 \text{ cmH}_2\text{O}$ of PEEP. The ventilatory profile was configured with $T_{\text{inspiration}}=0.25 \text{ s}$, $T_{\text{pause}}=0.1 \text{ s}$ and $T_{\text{expiration}}=0.4 \text{ s}$ to provide an end-inspiratory pause that matched the 100 ms exposure length and minimized image motion artifacts. Doses were delivered via a heat-thinned PE10 polyethylene cannula placed inside the ET tube so that its tip extended 5 mm below the end of the ET tube,³³ a similar depth to that used in our mouse lung gene transfer studies.¹ The same UltraMicroPump III syringe was used to remotely deliver the contrast mix via this smaller cannula.

Image capture was triggered by the ventilator at the beginning of every end-inspiratory pause, that is, every 1.33 s. After 15 s of baseline collection (20 breaths), a 15 μl sample of the contrast mix (surrogate of LPC or vector) was delivered in a single bolus over 30 s. This dose volume has been used in our lung gene transfer studies.¹ After 20 min, a second bolus of 15 μl was delivered over 3.6 s (the maximum rate of the syringe pump) to assess the effects of rapid delivery. Imaging continued for a further 4 min creating a 24 min data set, consisting of a total of 1920 images per mouse.

Post-experimental analyses

Each image sequence was flat-field and dark-field corrected and an image subtraction algorithm was used to locate changes in image brightness (Matlab R 2009b, The Mathworks, Natick, MA, USA). For the nasal studies, the brightness difference was calculated by subtracting each frame from the baseline image five frames before delivery initiation (that is, background subtraction of the mouse anatomy to reveal the fluid motion). A constant threshold of 128 gray values (1/32 the dynamic range) was then applied to select only the large intensity changes likely to correspond to fluid motion. The results were then 3×3 median filtered to reduce noise before being used to pseudo-color the original images to show the presence and/or movement of the delivered fluid. The regions where the image became darker (increasing presence of contrast fluid) were colored with a red to yellow color scale, and those that became lighter (decreasing presence of contrast fluid) were colored with a blue to purple color scale (see Figure 1). For the lung studies, the brightness difference between successive frames (that is frame differencing) was calculated to compensate for the greater confounding movements produced by the constant respiratory and cardiac motion. Each frame was converted to an RGB image and the red, green and blue channels were adjusted to show the regions with more contrast fluid in yellow and the regions with less contrast fluid as light blue. This visualization method minimized the effects of body motion and eliminated the need to choose a different threshold for each animal that would complicate between-animal comparisons. For high-quality motion-detection analysis, the background must remain still compared with the foreground objects (here, the contrast fluid) to be detected, hence the special efforts we made to minimize the movement of the mouse during imaging, including the use of restraining boards and respiratory gating as described above.

CONFLICT OF INTEREST

The authors declare no conflict of interest.

ACKNOWLEDGEMENTS

This study was supported by the NH&MRC Australia, with additional support from philanthropic donors via the CURE4CF Foundation (<http://www.cure4cf.org>). The synchrotron radiation experiments were performed on the BL20B2 beamline at SPring-8, with the approval of the Japan Synchrotron Radiation Institute (JASRI) under proposal number 2010A1523. Professor Naoto Yagi and Dr Kentaro Uesugi provided expert synchrotron imaging and controls advice and assistance at the SPring-8 synchrotron. We thank P Cmielewski, M Limberis and D Miller for their editorial input. MD, KS, AJ and DP were supported by the International Synchrotron Access Program (ISAP) managed by the Australian Synchrotron. The ISAP is an initiative of the Australian Government being conducted as part of the National Collaborative Research Infrastructure Strategy.

AUTHOR CONTRIBUTIONS

DP conceived the research; MD and DP devised the experiments; MD and DP performed the animal experiments in conjunction with KS and AJ who performed the synchrotron imaging; MD and DP conceived the image analyses; MD performed the image analyses and constructed the figures and Supplementary Material; MD and DP wrote the initial manuscript and all authors edited and approved the final version.

- Liu C, Wong E, Miller D, Smith G, Anson D, Parsons D. Lentiviral airway gene transfer in lungs of mice and sheep: successes and challenges. *J Gene Med* 2010; **12**: 647–658.
- Stocker A, Kremer K, Koldej R, Miller D, Anson D, Parsons D. Single-dose lentiviral gene transfer for lifetime airway gene expression. *J Gene Med* 2009; **11**: 861–867.
- Cmielewski P, Anson DS, Parsons DW. Lysophosphatidylcholine as an adjuvant for lentiviral vector mediated gene transfer to airway epithelium: effect of acyl chain length. *Respir Res* 2010; **11**: 84.

- Limberis M, Anson DS, Fuller M, Parsons DW. Recovery of airway cystic fibrosis transmembrane conductance regulator function in mice with cystic fibrosis after single-dose lentivirus-mediated gene transfer. *Hum Gene Ther* 2002; **13**: 1961–1970.
- Griesenbach U, Boyd AC. Pre-clinical and clinical endpoint assays for cystic fibrosis gene therapy. *J Cyst Fibros* 2005; **4**: 89–100.
- Griesenbach U, Smith SN, Farley R, Singh C, Alton EW. Validation of nasal potential difference measurements in gut-corrected CF knockout mice. *Am J Resp Cell Mol* 2008; **39**: 490–496.
- Soto-Montenegro ML, Conejero L, Vaquero JJ, Baeza ML, Zubeldia JM, Desco M. Assessment of airway distribution of transnasal solutions in mice by PET/CT imaging. *Mol Imaging Biol* 2009; **11**: 263–268.
- Cloetens P, Barrett R, Baruchel J, Guigay JP, Schlenker M. Phase objects in synchrotron radiation hard X-ray imaging. *J Phys D: Appl Phys* 1996; **29**: 133–146.
- Snigirev A, Snigireva I, Kohn V, Kuznetsov S, Schelokov I. On the possibilities of X-ray phase contrast microimaging by coherent high-energy synchrotron radiation. *Rev Sci Instrum* 1995; **66**: 5486–5492.
- Parsons DW, Morgan K, Donnelley M, Fouras A, Crosbie J, Williams I *et al*. High-resolution visualization of airspace structures in intact mice via synchrotron phase-contrast X-ray imaging (PCXI). *J Anat* 2008; **213**: 217–227.
- Siu KKW, Morgan KS, Paganin DM, Boucher R, Uesugi K, Yagi N *et al*. Phase contrast X-ray imaging for the non-invasive detection of airway surfaces and lumen characteristics in mouse models of airway disease. *Eur J Radiol* 2008; **68**: S22–S26.
- Donnelley M, Morgan K, Fouras A, Skinner W, Uesugi K, Yagi N *et al*. Real-time non-invasive detection of inhalable particulates delivered into live mouse airways. *J Synchrotron Radiat* 2009; **16**: 553–561.
- Donnelley M, Morgan K, Skinner W, Suzuki Y, Takeuchi A, Uesugi K *et al*. A new technique to examine individual particle and fibre deposition and transit behaviour on live mouse trachea. *J Synchrotron Radiat* 2010; **17**: 719–729.
- Sinn PL, Arias AC, Brogden KA, McCray PB. Lentivirus vector can be readministered to nasal epithelia without blocking immune responses. *J Virol* 2008; **82**: 10684–10692.
- Mitomo K, Griesenbach U, Inoue M, Somerton L, Meng CX, Akiba E *et al*. Toward gene therapy for cystic fibrosis using a lentivirus pseudotyped with sendai virus envelopes. *Mol Ther* 2010; **18**: 1173–1182.
- Hart D, Hillier MC, Wall BF. National reference doses for common radiographic, fluoroscopic and dental X-ray examinations in the UK. *Br J Radiol* 2009; **82**: 1–12.
- Kitchen MJ, Paganin D, Lewis RA, Yagi N, Uesugi K, Mudie ST. On the origin of speckle in X-ray phase contrast images of lung tissue. *Phys Med Biol* 2004; **49**: 4335–4348.
- Grubb BR, Boucher RC. Pathophysiology of gene-targeted mouse models for cystic fibrosis. *Physiol Rev* 1999; **79** (1 Suppl): S193–S214.
- Chandler SG, Illum L, Thomas NW. Nasal absorption in the rat. 1. A method to demonstrate the histological effects of nasal formulations. *Int J Pharmaceut* 1991; **70**: 19–27.
- Sinn PL, Burnight ER, Hickey MA, Blissard GW, McCray Jr PB. Persistent gene expression in mouse nasal epithelia following feline immunodeficiency virus-based vector gene transfer. *J Virol* 2005; **79**: 12818–12827.
- Mery S, Gross EA, Joyner DR, Godo M, Morgan KT. Nasal diagrams—a tool for recording the distribution of nasal lesions in rats and mice. *Toxicol Pathol* 1994; **22**: 353–372.
- Cmielewski P, Anson DS, Parsons DW. Re-emergence of luciferase expression in lung following a single nasal instillation of a lentiviral vector in normal and cystic fibrosis mice. *J Cyst Fibros* 2010; **9**(S1): S17.
- Grubb BR, Rogers TD, Boucher RC, Ostrowski LE. Ion transport across CF and normal murine olfactory and ciliated epithelium. *Am J Physiol Cell Physiol* 2009; **296**: C1301–C1309.
- Boone JM, Velazquez O, Cherry SR. Small-animal X-ray dose from micro-CT. *Mol Imaging* 2004; **3**: 149–158.
- Figueras SD, Winkelmann CT, Miller WH, Volkert WA, Hoffman TJ. TLD assessment of mouse dosimetry during microCT imaging. *Med Phys* 2008; **35**: 3866–3874.
- Griesenbach U, Munkonge FM, Sumner-Jones S, Holder E, Smith SN, Boyd AC *et al*. Assessment of CFTR function after gene transfer *in vitro* and *in vivo*. *Methods Mol Biol* 2008; **433**: 229–242.
- Gallotti A, Uggeri F, Favilla A, Cabrini M, de Haen C. The chemistry of iomeprol and physico-chemical properties of its aqueous solutions and pharmaceutical formulations. *Eur J Radiol* 1994; **18** (Suppl 1): S1–S12.
- Iomeron Data Sheet. From: Eisai Co., Ltd, Japan, 2009, http://www.eisai.jp/medical/products/di/EPI/IOM_V_EPI.pdf.
- Griesenbach U, Meng C, Farley R, Wasowicz MY, Munkonge FM, Chan M *et al*. The use of carboxymethylcellulose gel to increase non-viral gene transfer in mouse airways. *Biomaterials* 2010; **31**: 2665–2672.
- Sinn PL, Shah AJ, Donovan MD, McCray Jr PB. Viscoelastic gel formulations enhance airway epithelial gene transfer with viral vectors. *Am J Resp Cell Mol* 2005; **32**: 404–410.
- Goto S, Takeshita K, Suzuki Y, Ohashi H, Asano Y, Kimura H *et al*. Construction and commissioning of a 215-m-long beamline at SPring-8. *Nucl Instrum Meth A* 2001; **467**: 682–685.
- Yabashi M, Yamazaki H, Tamasaku K, Goto S, Takeshita K, Mochizuki T *et al*. SPring-8 standard X-ray monochromators. *Proc SPIE* 1999; **3773**: 2–13.
- Donnelley M, Parsons D, Morgan K, Siu K. Animals in synchrotrons: overcoming challenges for high-resolution, live, small-animal imaging. *AIP Proc* 2010; **1266**: 30–34.

Supplementary Information accompanies the paper on Gene Therapy website (<http://www.nature.com/gt>)